Interannual to Decadal Variability of Atlantic Water in the Nordic and Adjacent Seas

James A. Carton[1], Gennady A. Chepurin[1], James Reagan[1], and Sirpa Häkkinen[2]

March 3, 2011

Revised May 10, 2011

Second revision September, 6, 2011

[1]Department of Atmospheric and Oceanic Science
University of Maryland, College Park, Maryland, USA

[2]NASA Goddard Space Flight Center, Greenbelt, Maryland, USA

Abstract

Warm salty Atlantic Water is the main source water for the Arctic Ocean and thus plays an important role in the mass and heat budget of the Arctic. This study explores interannual to decadal variability of Atlantic Water properties in the Nordic Seas area where Atlantic Water enters the Arctic, based on a reexamination of the historical hydrographic record for the years 1950-2009, obtained by combining multiple data sets. The analysis shows a succession of four multi-year warm events where temperature anomalies at 100m depth exceed 0.4^{o}C, and three cold events. Three of the four warm events lasted 3-4 years, while the fourth began in 1999 and persists at least through 2009. This most recent warm event is anomalous in other ways as well, being the strongest, having the broadest geographic extent, being surface-intensified, and occurring under exceptional meteorological conditions. Three of the four warm events were accompanied by elevated salinities consistent with enhanced ocean transport into the Nordic Seas, with the exception of the event spanning July 1989-July 1993. Of the three cold events, two lasted for four years, while the third lasted for nearly 14 years. Two of the three cold events are associated with reduced salinities, but the cold event of the 1960s had elevated salinities. The relationship of these events to meteorological conditions is examined. The results show that local surface heat flux variations act in some cases to reinforce the anomalies, but are too weak to be the sole cause.

1. Introduction

The recent dramatic warming of Arctic Ocean surface temperatures and shrinkage of sea ice coverage have been accompanied by a warming and salinification of the Atlantic Water Mass flowing into the Nordic Seas from the Atlantic (*Holliday et al., 2008*; *Piechura and Walczowski, 2009*; *Matishov et al., 2009; Dmitrenko et al., 2008, 2009*). Warmings of this water mass have also occurred in the 1920s-1930s, 1960s, 1970s, and 1990s (*Swift et al., 2005; Levitus et al., 2009a; Matishov et al, 2009*) raising the question of how different the recent warming is from past warmings. As a contribution to addressing this question we revisit the interannual-to-decadal variability of the Atlantic Water mass in the Nordic Seas during the past 60 years and its relationship to hemispheric climate variability using a single combined hydrographic data set that builds on the newest release of the World Ocean Database (*Boyer et al., 2009*).

The Nordic Seas is the region north of the Greenland-Scotland Ridge and south of the Arctic Ocean, including the fairly shallow Barents, and deep Norwegian, Iceland, and Greenland Seas (*Hansen and Osterhus, 2000*) (**Fig. 1**). The inflow of the Atlantic Water, which is characterized by warm temperatures and high salinity, occurs via three main branches: approximately 1Sv (=10^6 m^3s^{-1}) passes west of Iceland in the North Icelandic Irminger Current, approximately 3.3-3.5Sv travels over the Iceland Faroe Ridge in the Faroe Current and approximately 3.7Sv passes in the form of inflow through the Faroe Shetland Channel (see *Hansen and Osterhus, 2000; Hansen et al, 2003* and references therein). The two western branches are mainly fed by water from the North Atlantic

Current while inflow through the Faroe Shetland Channel is mainly the warmer and more saline Eastern North Atlantic Water (e.g. *Hakkinen and Rhines, 2009; Hakkinen et al., 2011a)*. Flow in the eastern branches merge towards the Norwegian coast in the Norwegian Sea, but retain two distinct cores (*Mork and Blindheim, 2000; Orvik and Niiler, 2002; Holliday et al. 2008*).

This flow branches with one branch of approximately 1.1 to 1.7Sv travelling eastward into the Barents Sea, and the other flowing northward in the West Spitsbergen Current through Fram Strait (*Ingvaldsen et al., 2004; Skagseth et al., 2008*). In the vertical it extends from a maximum of 600m depth to the base of the Arctic Surface Water. As this Atlantic Water is transported poleward its properties are altered through mixing so that temperature and salinity classes vary significantly by location. In the shallow Barents Sea cooling and freshening leads to an approximately linear relationship between temperature and salinity ranging from 8^{o}C and 35.13 psu down to 0^{o}C and 34.87psu or colder (*Schauer et al., 2002; Smolyar and Adrov, 2003*). At Fram Strait *Schauer et al. (2004)* define a minimum temperature for Atlantic Water (>1^{o}C), *Schlichtholz and Goszczko (2006)* define both temperature and salinity minimums (>2^{o}C and >34.9psu), *Saloranta and Haugan (2001)* and *Piechura and Walczowski (2009)* make similar choices (>0^{o}C, >34.93psu), while *Marnela et al. (2008)* define a density range (σ_θ =27.70 to 27.97). For this study we define the Atlantic Water Zone (AWZ) as the geographic region circumscribed by the time mean 35psu contour at 100m depth north of 63^{o}N, (see **Fig.1**). The southern limit of this domain is chosen to exclude most of the ocean south of the Iceland-Faroe Ridge from these calculations. Calculations are done over a depth range of 0/600m which spans the depth range of the Atlantic Water in this region. The data coverage is insufficient to allow more sophisticated isopycnal or isohaline analyses.

Superimposed on seasonal variations in transports and stratification (e.g., *Ingvaldsen et al., 2004*), Atlantic Water properties undergo strong interannual to decadal variations. One of the best continuous records is available at Ocean Weather Station M, maintained in the Norwegian Sea (66^{o}N, 2^{o}E) since 1948. The Station M record shows a warming trend at the surface and a decadal succession of warmings at the surface and in the 50-200m layer in the early 1960s, and the early to mid-1970s, (*Blindheim et al 2000; Polyakov et al., 2004*). The transition from warm, salty conditions of the early to mid-1970s to cooler and fresher conditions of the Great Salinity Anomaly appears dramatically in this region during 1976-1981 (*Dickson et al., 1988).* Further discussion of this remarkable event is available in *Belkin et al. (1998)* and *Belkin (2004*). Warm conditions returned in early 1990s followed by cooling in the mid-1990s. Many of these warmings are associated with enhanced salinity superimposed on a multi-decadal freshening trend. The Kola Bay meridian transect (lying along the 33^{o}E meridian) offers another long time series record of conditions within the Barents Sea extending back to the beginning of the 20th century and, among other features, delineating the 1920s-1930s warming (*Matishov et al, 2009*). Since 1960 the time series suggests that along this meridian there were also a set of warm events in the 1960s, early to mid-1970s, 1983-4, and 1989-1994, and the 2000s with prominent cold events in the late-1960s, late-1970s, and late-1990s. *Saloranta and Haugan (2001) and Polyakov et al (2004)* describe a time series for the region northwest of Svalbard that also shows variability on similar time scales.

To complement these rare time series observations, a number of studies have examined conditions during specific years. The early 1960s event appears at coarse resolution in the Environmental Working Group survey described in *Swift et al. (2005).* Interestingly, the modeling study of *Gerdes et al. (2003)* suggests this event to be the result of the impact of a melt-induced halocline on net surface heat loss.

Furevik (2000; 2001) and *Saloranta and Haugan (2001)* track spatial aspects of heat anomalies for the warm and cold events of the 1980s and 1990s. These studies make the case for the importance of ocean advection in giving rise to the 1983-1984 warm event and the 1986-1988 cold event, but argue that the 1990-1992 warm event may be most closely related to changes in surface flux. *Furevik (2000)* also introduces the use of observations of SST to track subsurface temperature anomalies.

Studies of the warming which has developed since 1999 have shown this latter to be dramatic (certainly the strongest warming since the 1930s) and also to have characteristics, such as its vertical structure, which set it apart from previous warmings (*Matishov et al., 2009*). *Walczowski and Piechura (2006), and Dmitrenko et al. (2008)* identify indications of anomalous temperature advection through Fram Straits and also through the Barents Sea into the northern Laptev Sea. Based on observations at Fram Strait *Schauer et al. (2004)* ascribe the advective cause of the warming to both increasing temperatures of the source waters and to increases in volume transport rates. Consistent with this, *Hakkinen and Rhines (2009)* examine surface currents in the source waters of the subpolar gyre and identify the presence of anomalous poleward advection of warm and saline waters.

The processes giving rise to these warm and cold events have been examined in many modeling studies (*Zhang et al. 1998; Karcher et al, 2003; Hu et al., 2004; Mauritzen, et al., 2006; Sando and Furevik, 2008; and Semenov et al., 2009*). The models with specified meteorology show significant ability to reproduce past anomalies in the Nordic Seas. Analysis of the results generally highlights the importance of changes in rate of advection of Atlantic Water entering the Nordic Seas.

This conclusion regarding the importance of ocean advection has also been used to explain an observed relationship between the December-February North Atlantic Oscillation (NAO) Index of winter sea level pressure and the temperature anomalies in the Nordic Seas (*Swift et al., 1998; Grotefendt et al., 1998; Dickson et al., 2000; Mork and Blindheim, 2000; Saloranta and Haugan, 2001; Polyakov et al., 2004; Furevik and Nilsen, 2005; and Schlichtholz and Goszczko, 2006*). However, the recent warming which has occurred under fairly neutral NAO conditions is an example of a situation when the relationship breaks down. *Bengtsson et al. (2004)* and *Sando and Furevik (2008)* propose that the key meteorological parameter is the local winds in the narrow zone between Spitsbergen and Norway. They argue, following *Zhang (1998),* that it is only these local winds which drive Atlantic Water transport into the Barents Sea thus increasing the spread of Atlantic Water (see also *Dmitrenko et al., 2009*). *Häkkinen et al. (2011*) show evidence to suggest that winter meteorological conditions over the subtropical gyre are an additional factor contributing to warming by forcing anomalous quantities of Atlantic Water into the Nordic Seas. This basin-scale contribution reached a peak around 1990 suggesting that this effect may have been important for the early 1990s warming. In a coupled modeling study *Semenov et al. (2009)* suggest that sea ice and surface heat flux changes also play a role in a feedback cycle associated with these transport variations.

This study is an effort to reexamine the spatial and temporal structure of the anomalies of Atlantic Water in the Nordic Seas with a combined hydrographic data set and then use the results to explore their relationship to atmospheric variables for the years since 1950.

2. Methods

This study relies foremost on the set of 420,199 temperature profiles and 258,912 salinity profiles (60^oN-90^oN, 50^oW-80^oE) in the National Oceanographic Data Center's World Ocean Database 2009 (WOD09, *Boyer et al., 2009*), including all instrument types which measure temperature or salinity, for the sixty-year period 1950-2009. The version used here is the standard level data which includes quality control carried out by the National Oceanographic Data Center. We have also applied a secondary quality check (including: checks for static stability, profile depth, buddy-check, and comparison to climatological profiles) which eliminates 3% of the salinity profiles and 1.8% of the temperature profiles. In addition to the WOD data we include all observations from the International

Council of the Exploration of the Seas database (approximately 50,000 unique profiles), the Woods Hole Oceanographic Institution Ice-Tethered Profile data, the North Pole Environmental Observatory data, and the Nansen and Amundsen Basin Observational System data (just a handful in our domain).

Many of the additional profiles were duplicates, but after eliminating these the additions increase our basic temperature data set by 58,469 profiles to a total of 478,668 temperature profiles, and the basic salinity data set by 52,314 profiles to 311,226 profiles, with the greatest increases in the northern North Atlantic and Barents Sea. The data set does contain some Expendable Bathythermograph temperature profiles, which are known to contain a time-dependent warm bias, notably during the 1970s. WOD09 contains a correction for this bias based on the work of *Levitus et al. (2009b)* which seems to remove it as an area of concern for this study.

The resulting observation distribution shows increases in coverage in the 1950s due to the introduction of drifting stations as well as aircraft and submarine surveys, and again in the 1980s due to a succession of scientific experiments (**Fig. 2**). Seasonally, the number of temperature observations peaks in summer at nearly 800 per month reducing to only 250 per month in winter.

All temperature and salinity profiles that are not already on standard levels are first interpolated to National Oceanographic Data Center standard levels using linear interpolation. After a simple set of quality controls the data are binned into

1^ox1^ox1month bins. To check the data set we have computed monthly climatologies of temperature and salinity and compared them to the monthly climatology to the Polar science center Hydrographic Climatology PHC3.0 (*Steele et al., 2001*). This new climatology is generally consistent with PHC3.0, but with some persistent patterns of $\pm 0.5^oC$ temperature and ± 0.1psu salinity differences on 100km scales in the upper 200m. We believe these differences result from the use in the current study of a more extensive data set with a more recent time-centering than PHC3.0 (which was based only on data collected prior to 1998). A simple *Cressman (1959)* gridding scheme is used to smooth the results in order to present the results graphically. Anomalies of AWZ heat content are evaluated by computing the volume integral of temperature times its heat capacity in the upper 600m of the AWZ, removing the time mean and smoothing with a two-year filter. Later we will identify warm and cold events as those that exceed $\pm 2 \times 10^{20}$J.

Because of persistent limitations of the spatial coverage of the hydrographic data set we complement our examination of hydrography by also examining the monthly NOAA/National Climate Data Center OI SST v2. The OI SST data set is based on satellite infrared emissivity and is available at 0.5^ox0.5^o resolution daily for the period January 1982 to December 2010 (*Reynolds et al., 2007*). While its spatial coverage is excellent OI SST is subject to potential sources of bias including: undetected stratus clouds and aerosol effects, unresolved diurnal effects, as well as error in interpretation of OI SST as if it were a measurement of bulk SST. These errors are particularly a concern during the years 1995-2002 due to problems with the satellite instruments (*Podesta et al., 2003*).

To evaluate the bias in OI SST, monthly binned temperature observations at 10m depth (deep enough to eliminate diurnal effects) throughout the domain 60°N-90°N, 50°W-80°E were matched with collocated monthly average OI SST observations for the years 1982-2009. Examination of these temperature differences reveals a temperature-dependent systematic 1°C warm bias in OI SSTs for SSTs cooler than 2°C becoming a 0.5-1.0°C cold bias for SSTs above 4°C. After removal of this bias through a simple geographical, and temperature-independent correction, the recomputed analysis of collocated monthly SST differences shows a ±2°C essentially random difference suggesting that this corrected monthly average OI SST should provide an unbiased estimate of bulk SST with an accuracy in the range of previous estimates (e.g. *Key et al., 1997*).

Finally, when examining the causes of anomalous rate of heat storage in the Nordic Seas we compare to four estimates of net surface heat flux. Three are based on atmospheric reanalyses: the National Centers for Environmental Prediction/National Center for Atmospheric Research (NCEP/NCAR) reanalysis of *Kalnay et al. (1996),* which covers the full period of this study; the European Centers for Medium Range Weather Forecasts ERA-40 analysis (*Uppala et al, 2005*), which covers the period 1958-2001; and the updated ERA-Interim, which spans the period 1989-2009 (*Dee and Uppala, 2009*). The fourth we consider is the Woods Hole Oceanographic Institution OAFlux/ISCCP analysis of *Yu et al. (2008)*, which is based on a combination of other products, weighted to match observations, and is available for the period 1983-2007. The first three also provide individual radiative and thermodynamic flux components.

3. Results

The time-mean horizontal structure of temperature and salinity at 100m shows a strong positive relationship between temperature and salinity due to the presence of an intrusion of warm salty Atlantic water and its gradual dilution. Interestingly, and helpfully for this study, the geographic location of this Atlantic Water is readily identified by the area defined by the 35psu isohaline (the AWZ), which remains generally stable with time. The shape of the AWZ reflects the fact that there is poleward path into the Nordic Seas (A-B on **Fig. 1**) which then branches with the northward branch passing through Fram Strait (B-C) and an eastward branch extending into the Barents Sea (B-D). The eastward branch shows more rapid cooling with distance than the northward branch and significant freshening as well.

The vertical structure of temperature and salinity along path A-B shows a subsurface salinity maximum with a core depth of 100-200m and a layer thickness that increases from less than 400m at point A to nearly 600m by point B, now generally overlain by cold, fresh surface water (**Fig. 3**). Interestingly, examination of the spatial structure of this overlying fresh surface layer suggests that it thins or disappears in a narrow band overlying the central core of the Atlantic Water between A-B. Along this path the high salinity (>35psu) layer approximately corresponds to a density range of 27.25-27.85 kg m^{-3} and a temperature range of 2^oC-9^oC. Along the northward branch (B-C) densities increase by approximately 0.25 kg m^{-3} while temperatures cool to below 5^oC. Along the eastward branch (B-D) density also increases by 0.25 kg m^{-3}, but the temperature cools even more and salinities drop below 35psu. The complexity of these water mass changes explains the multiple regionally-dependent definitions of Atlantic Water described in the *Introduction*. Seasonal changes are most pronounced in the surface layer (**Fig. 1** insets).

We next examine the variability of temperature and salinity anomalies about their monthly climatology, averaged spatially throughout the AWZ, and annually averaged with a 12-month running filter in **Fig. 4** to eliminate seasonal variability and increase statistical confidence. The relatively shallow Barents Sea means that the horizontal extent of the integrals vary with depth. The record reveals that since 1950 there have been four distinct warm events spanning multiple years: July 1959-July 1962, October 1971- August 1975, July 1989-July 1993, and March 1999- December 2009 and beyond, which we label W1-W4 (emulating the notation of *Furevik, 2001*). In-between these we find three cold events: April 1965- February 1969, July 1976- January 1989, and August 1994- March 1998 which we label C1-C3. As discussed in the *Introduction* each of these events have also been identified in other observational studies.

W1 (1959-1962) first appears as a 0.3^{o}C nearsurface warm temperature and 0.04 psu high salinity anomaly in late 1959 whose density effects nearly compensate (**Fig. 4**). The temperature anomaly rapidly deepens to 500m and then more gradually to 1000m (well below the layer containing the Atlantic Water core) by 1964, accompanied by a similar deepening of the salinity anomaly. Examination of the spatial structure of the anomaly (**Fig. 5**) shows the temperature and salinity anomalies to be most pronounced in the south, extending into the Barents Sea, beyond the AWZ towards

Novaya Zemlya. Lack of data coverage limits our ability to see the northward extension of this event.

C1 (1965-1969) is a -0.3°C cold anomaly that persists until early 1969 when salinities increase throughout the upper 800m by more than 0.04psu. As a result of this cooling and salinification, stratification in the upper ocean above 400m weakens significantly throughout the late-1960s and early 1970s and potential density increases by 0.04kg m^{-3}. An examination of the spatial structure of this event shows the maximum cold anomaly to be in the Norwegian Sea south of Svalbard while the salinity anomaly is displaced further southward (**Fig. 6**). The eastward extent of either is unknown due to limitations in data coverage during this decade.

W2 (1971-1975) has a deeper structure than W1 with a maximum temperature anomaly between 600-700m depth and a correspondingly deep, but weak, positive salinity anomaly (indeed, the salinity anomaly precedes this warm event). Geographically, the deep temperature anomaly primarily occurs east of Iceland with shallower temperature anomalies extending into the Barents Sea, while the positive salinity anomaly is most pronounced in the Barents Sea at a time when the subpolar gyre is anomalously fresh (**Fig. 5**).

C2 (1976-1989) is the longest lasting anomaly considered here (13 years), but the major cold anomaly occurs during the first four years, a part of the event which has been associated in the literature (e.g. *Dickson et al., 1988; Belkin et al., 1998*) with the return of the Great Salinity Anomaly to the Nordic Seas. During these early years temperatures between 0/300m decrease by more than -0.45°C and salinities decrease by more than -0.08psu. As in the case of W1 these temperature and salinity anomalies nearly compensate so the impact on density and thus stratification is weak. This cold/fresh anomaly has broad spatial structure, spanning much of our domain (**Fig. 6**). During the later years of C2 temperatures in the upper 500m remain anomalously cool, but with only weak salinity anomalies so that surface density increases. C2 represents a transition point in our record in that the water column is significantly more stable in the years following 1989 than in prior years due to the persistence of the freshening which began in the late-1970s.

W3 (1989-1993) is a five-year long 0.3°C warming of the upper 500m, but as there is no compensating salinity anomaly its effect on increasing the stratification of the base of the Atlantic Water was substantial. This warm anomaly is most pronounced west of the Barents Sea Opening and throughout the Barents Sea at a time when the subpolar gyre is anomalously cool (**Fig. 5**). In contrast to the other warm events W3 is associated with reduced salinities throughout much of the domain except along the southern Norwegian coast.

C3 (1994-1998) is a short-lived but 700m deep weak cold/fresh event which is density compensated. The spatial structure of this anomaly is not well-defined due to limitations of the hydrographic sampling during the 1990s, however the anomaly appears to extend at least partway into the Barents Sea (**Fig. 6**).

W4 (1999-2009+) is a strong, surface intensified warm event with temperature anomalies in the upper 300m that exceed 0.45°C. This warming occurs throughout the Nordic Seas except Denmark Strait and is accompanied by a similarly broad, but weak salinity anomaly (**Fig. 5**). As a result W4 is associated with significantly enhanced stratification with surface density decreasing by 0.045kg m^{-3}.

The surface intensification of the temperature anomaly associated with W4 (e.g. **Fig. 4)** allows us to use SST to examine its basin-scale and detailed temporal structure (**Fig. 7**). SST shows that the warming spans the entire northern North Atlantic sector including such marginal seas as the North Sea and the Baltic, but is more pronounced in the western side of the Atlantic basin than the central/east. The SST also shows that warming is present in both winter and summer, although it is less pronounced in marginal seas in winter. In contrast, in the Barents Sea the warm anomaly is less evident in summer, perhaps due to capping by low salinity Surface Water. Averaged over the extended domain (60^oW-80^oE, 40^oN-90^oN, excluding marginal seas) the anomaly was quite prominent in the summers of 2001 and 2003, but then remains quite warm both winter and summer from 2005-2008. In 2009 it is reduced, but in 2010 the SST anomaly returns in intensified form.

As discussed in the *Introduction* both advective effects and variations in surface heating have been suggested as causes of temperature anomalies in the Nordic Seas. We explore the potential contribution of anomalies of surface heat flux over the AWZ itself by first computing anomalous AWZ heat content in the upper 600m and then differentiating this quantity to obtain rate of heat storage (**Fig. 8**). The time series of 0/600m heat content shows each of the warm and cold events identified above exceed $\pm 2x10^{20}$J (equivalent to[1] a 0/600m average temperature anomaly of $\pm 0.12^oC$). The record maximum heat content anomaly of $>1x10^{21}$J occurs at the peak of warming associated with W4 in early

[1] A reviewer notes that the observations of Piechura and Walczowski (2009) are in the West Spitsbergen Current which typically lags the southern Norwegian Sea and Faroe Shetland Channel by 1-4 years.

2005 (a year before the peak appears in the AREX cruise data of *Piechura and Walczowski, 2009* and more than a year before the peak in SST) while the minimum of < $-9x10^{20}$J occurs during C2 in 1979. Interannual variations in rate of heat storage fall in the range of $\pm 20Wm^{-2}$.

It is evident from comparison of the time series (**Fig. 8** upper panel) that the NAO Index (either annual or DJF) is an uneven predictor of warming of the AWZ. W1, W2 and W3 are all associated with positive values of the NAO Index as well as positive wind stress curl anomalies over the Atlantic Water domain (although we note that W3 is not associated with high salinities). Cold event C1 is associated with a negative NAO Index anomalies, but not with low salinities, while C2 and C3 do not seem to be associated with extrema of the NAO Index. We anticipate that the impact of NAO on the AWZ is strongly modulated by local forcing associated with the appearance of anomalous westerly winds in the Barents Sea, reminiscent of the suggestion of local forcing by *Bengtsson et al. (2004)* and *Sando and Furevik (2008)*.

Finally, we consider the direct effect of meteorological conditions on net surface heat flux by comparing anomalous rate of heat storage in the AWZ to anomalous net surface heat flux averaged over the AWZ. Four anomalous flux estimates considered here differ from each other by a substantial ± 5-$10Wm^{-2}$. However, some common features are evident. Of the two surface flux estimates that span multiple decades NCEP/NCAR has significantly larger anomalies than ERA-40. Examination of the individual flux components in both data sets shows an increased sensible heat flux of up to 10 Wm^{-2} due to warm air advection. Despite these differences in amplitude, the phases of the anomalies in the two products are in reasonable agreement with each other and both are too small by a factor of 2-3 to explain the heat storage anomalies. We conclude that heat flux offers a weak positive contribution to heat storage (with heat flux anomalies lagging heat storage anomalies somewhat).

A similar conclusion can be drawn from the combined set of four flux estimates for the more recent two decades when all are available. Arond 1990, for example, the surface flux estimates show that net downward surface heat flux increases for several years. Examination of the individual flux components shows this increase is due to an increase of sensible heat flux of up to $10 Wm^{-2}$ due to warm air advection. But, this surface flux anomaly is too small by a factor of two to explain the increase in heat storage, an explanation which had been proposed by *Overland et al. (2008*). Other factors such as wind-induced changes in the rate of Atlantic Water entering the Nordic Seas (discussed above and inferred in **Fig. 8** lower panel from the difference between storage and surface flux) must be invoked to explain these heat storage anomalies.

4. Summary

Here we report on a reexamination of subseasonal anomalies of Atlantic Water in the Nordic Seas area of the Arctic Mediterranean for the 60-year period 1950-2009 using a combined set of hydrographic observations drawn from several data sets. The reexamination reveals a succession of four warm and three cold events during this period which exceed a threshold of $\pm 2x10^{20}J$ in the Atlantic Water Zone for two years, W1: July

1959-July 1962, W2: October 1971- August 1975, W3: July 1989-July 1993, and W4: March 1999- December 2009 and beyond, C1: April 1965- February 1969, C2: July 1976- January 1989, and C3: August 1994- March 1998. Many of these events show that they extend eastward into the Barents and Kara Seas. Their extensions northward past Fram Straits are uncertain due to lack of data coverage. The events have other features in common. Warm events are generally characterized by elevated salinities (the exception is W3, July 1989-July 1993), while two of three cold events are characterized by reduced salinities. This positive relationship is consistent with the volumetric estimates *Levitus et al. (2009a)* in the Barents Sea, suggesting the importance of anomalous advection of Atlantic Water. Most of the events satisfying our definition persist for 3-4 years. The first of two exceptions is C2 which lasted 13 years. C2 is unusual because the main anomaly actually spans only the first four years and also because the event seems to have permanently increased stability of the water column by lowering salinity of the upper layer. The second exception is the recent and intense W4, spanning 1999 to the end of our analysis in 2009.

A number of previous studies have also examined multi-year variability of the properties of the Atlantic Water in this region, as reviewed in the *Introduction*. A notable study by Furevik (2001) uses observations from five hydrographic sections to consider variability during the 17-year period 1980-1996 relative to the mean of that period. Interestingly, this period begins just after the most intense part of C2 and ends just before the onset of the intense W4. One of the distinctions of these results from ours is that Furevik (2001) highlights a warm event during 1983-4 (also evident in the Kola Bay transect) which would fall in the middle of our second cold event C2. This 1983-4 warming is in fact also evident in our results (e.g. **Fig. 4**) but is of lower amplitude that other events in our record and thus does not meet our definition of a warm event.

In the second part of this paper we consider the relationship of the temperature anomalies in the Nordic Seas to changing meteorological conditions. As discussed in the *Introduction*, there is a (rather limited) relationship between these temperature anomalies and the NAO Index, which in turn is associated with a northward displacement of storm tracks as well as the strength of monthly mean westerlies in this region. Year to year changes in synoptic wind variability within this region may turn out to be a key additional variable (*Hakkinen et al. 2011b*). W4, which has occurred during a period of near-neutral annual NAO Index, is an example of a case where the Index is a poor predictor. A better predictor is the frequency of occurrence of wintertime atmospheric blocking events. We also explore the possibility that the temperature anomalies in the Nordic Seas may be explained by local anomalies of net surface heat flux, by comparing heat storage in the Atlantic Water Zone with four alternative estimates of net surface flux. We find that while the estimates are themselves not very consistent, they are all too small by a factor of 2-3 to explain the observed heat storage anomalies.

Having ruled out anomalies of net surface heat flux, our results support the results of a number of transport observation and modeling studies reviewed in the *Introduction* that suggest anomalous advection of Atlantic Water into the Nordic Seas as the more plausible explanation for the appearance of these anomalies (e.g. *Zhang et al., 1998*).

However, issues related to the underlying dynamics of this process and the potential role of interactions with the overlying atmosphere remain.

Acknowledgements

We are grateful to the NOAA Earth System Research Laboratory, Physical Sciences Division for access to their High Resolution SST data, (www.esrl.noaa.gov/psd/), to the NOAA National Oceanographic Data Center (www.nodc.noaa.gov), the International Council of the Exploration of the Seas (www.ices.dk*)*, the Woods Hole Oceanographic Institution Ice-Tethered Profile (www.whoi.edu/page.do?pid=20781) and Hydrobase II (www.whoi.edu/science/PO/hydrobase/) archives for providing access to their hydrographic data sets. Without their cooperation this work would not be possible. The anonymous reviewers significantly improved this manuscript. JAC, JR, and GAC gratefully acknowledge support by the National Science Foundation (OCE0752209). SH gratefully acknowledges the support of the NASA OSTM Physical Oceanography Program.

References

Belkin I.M., S. Levitus, J. Antonov, et al., 1998: "Great Salinity Anomalies" in the North Atlantic, Progr. Oceanogr., 41, 1-68.

Belkin, I.M., 2004: Propagation of the ‘‘Great Salinity Anomaly’’ of the 1990s around the northern North Antic, *Geophys. Res. Letts.*, **31**, L08306, doi:10.1029/2003GL019334.

Bengtsson, L., V.A. Semenov, and O.M. Johannessen, 2004: The early twentieth-century warming in the Arctic: A possible mechanism, *J. Clim.*, **17**, 4045 – 4057, doi:10.1175/1520-0442.

Blindheim, J., V. Borovkov, B. Hansen, S.-A. Malmberg, W.R. Turrell, and S. Osterhus, 2000: Upper layer cooling and freshening in the Norwegian Sea in relation to atmospheric forcing, *Deep-Sea Res. I*, **47**, 655-680.

Boyer, T.P., J. I. Antonov, O. K. Baranova, H. E. Garcia, D. R. Johnson, R. A. Locarnini, A. V. Mishonov, D. Seidov, I. V. Smolyar, and M. M. Zweng, 2009: World Ocean Database 2009, Chapter 1: Introduction, NOAA Atlas NESDIS 66, Ed. S. Levitus, U.S. Gov. Printing Office, Wash., D.C. , 216 pp., DVD.

Cressman, G.P., 1959: An Operational Objective Analysis System, *Mon. Wea. Rev.*, **87**, 367–374.

Dee, D. P., and S. Uppala, 2009: Variational bias correction of satellite radiance data in the ERA-Interim reanalysis. *Quart. J. R. Meteorol. Soc.*, **135**, 1830-1841.

Dickson, R.R., Meincke, J., Malmberg, S.-A., Lee, A.J., 1988. The Great salinity anomaly in the northern North Atlantic 1968-1982. Progress in Oceanography 20, 103-151.

Dickson, R.R., T.J. Osborn, J.W. Hurrell, J. Meincke, J. Blindheim, B. Adlandsvik, T. Vinje, G. Alexeev, and W. Maslowski, 2000: The Arctic Ocean response to the North Atlantic Oscillation, *J. Clim.*, **13**,2671–2696.

Dmitrenko, I.A., I.V. Polyakov, S.A. Kirillov, L.A. Timokhov, I.E. Frolov, V.T. Sokolov, H.L. Simmons, V.V. Ivanov, and D. Walsh, 2008: Towards a warmer Arctic Ocean: spreading of the early 21st century Atlantic water warmer anomaly along the Eurasian Basin margins. *J. Geophys. Res*., **113**, C05023.

Dmitrenko, I.A., D. Bauch, S. A.Kirillov, N. Koldunov, P.J. Minnett, V.V. Ivanov, J.A.Holemann, and L.A.Timokhov, 2009: Barents Sea upstream events impact the properties of Atlantic water inflow into the Arctic Ocean: Evidence from 2005 to 2006 down stream observations *Deep-Sea Res. I*, **56**, 513–527.

Furevik, T., 2000: On anomalous sea surface temperatures in the Nordic Seas, *J. Clim.*, **13**, 1044– 1053.

Furevik, T., 2001: Annual and interannual variability of Atlantic water temperatures in the Norwegian and Barents Seas: 1980–1996. *Deep-Sea Res. I*, **48**, 383–404.

Furevik, T. and J.E.O. Nilsen, 2005: Large-Scale Atmospheric Circulation Variability and its Impacts on the Nordic Seas Ocean Climate - a review, in The Nordic Seas: An Integrated Perspective, H. Drange, T. Dokken, T. Furevik, R. Gerdes and W. Berger, Eds., AGU Monograph 158, American Geophys. Union, Wash. DC, 105-136.

Gerdes R., M. J. Karcher, F. Kauker, and U. Schauer, 2003: Causes and development of repeated Arctic Ocean warming events, *Geophys. Res. Letts.*, **30**, 1980, doi:10.1029/2003GL018080.

Grotefendt, K., K. Logemann, D. Quadfasel, and S. Ronski, 1998: Is the Arctic Ocean Warming?, *J. Geophys. Res.*, **103**, 27,679-27,687.

Häkkinen, S., and P.B. Rhines, 2009: Shifting surface currents in the northern North Atlantic Ocean, *J. Geophys. Res.*, **114**, C04005, doi:10.1029/2008JC004883.

Häkkinen, S., P.B. Rhines, and D.L. Worthen, 2011a: Warm and saline events embedded in the meridional circulation of the northern North Atlantic, *J. Geophys. Res.*, **116**, C03006, doi:10.1029/2010JC006275.

Häkkinen, S., P.B. Rhines and D.L.Worthen, 2011b Atmospheric blocking and Atlantic multidecadal ocean variability, submitted.

Hansen, B., and S. Østerhus, 2000: North Atlantic–Nordic Seas exchanges, *Progr. Oceanogr.*, **45**, 109–208.

Hansen, B., S. Østerhus, H. Hatun, R. Kristiansen, and K.M.H. Larsen, 2003: The Iceland-Faroe inflow of Atlantic water to the Nordic Seas, *Progr. Oceanogr.*, **59**, 443-474.

Holliday, N. P., S. L. Hughes, S. Bacon, A. Beszczynska-Moller, B. Hansen, A. Lavın, H. Loeng, K. A. Mork, S. Østerhus, T. Sherwin, and W. Walczowski, 2008: Reversal of the 1960s to 1990s freshening trend in the northeast North Atlantic and Nordic Seas, Geophys. Res. Letts., 35, L03614, doi:10.1029/2007GL032675.

Hu, A., G.A. Meehl, W.M. Washington, and A. Dai, 2004: Response of the Atlantic Thermohaline Circulation to Increased Atmospheric CO_2 in a Coupled Model, *J. Clim.*, **17**, 4267-4279.

Ingvaldsen, R.B., L. Asplin, and H. Loeng, 2004: Velocity field of the western entrance to the Barents Sea, *J. Geophys. Res.*, **109**, C03021.

Kalnay, E. et al., 1996: The NCEP/NCAR 40-Year Reanalysis Project, *Bull. Amer. Meteor. Soc.*, **77**, 437-471.

Karcher, M. J., R. Gerdes, F. Kauker, and C. Köberle, 2003: Arctic warming: Evolution and spreading of the 1990s warm event in the Nordic seas and the Arctic Ocean, *J. Geophys. Res.*, **108**, 3034, doi:10.1029/2001JC001265.

Key J.R., J.B. Collins, C. Fowler, and R.S. Stone, 1997: high latitude surface temperature estimates from thermal satellite data, *Remote Sens. Environ*., **61**, 302-309.

Levitus, S., G. Matishov, D. Seidov, and I. Smolyar, 2009a: Barents Sea Multidecadal Variability, *Geophys. Res. Letts.* , **36**, L19604, doi: 10.1029/2009GL039847.

Levitus S., J.I. Antonov, T.P. Boyer, R.A. Locarnini, H.E. Garcia, and A.V. Mishonov, 2009b: Global ocean heat content 1955-2008 in light of recently revealed instrumentation problems, *Geophys. Res., Letts.*, **36,** L07608.

Marnela, M., B. Rudels, K. A. Olsson, L.G. Anderson, E. Jeansson, D.J. Torres, M.-J. Messias, J.H. Swift, and A.J. Watson, 2008: Transports of Nordic Seas water masses and excess SF6 through Fram Strait to the Arctic Ocean, *Progr. Oceanogr.*, **78**, 1–11.

Matishov G.G. Matishov, D.G. Matishov, and D.V. Moiseev, 2009: Inflow of Atlantic-origin waters to the Barents Sea along glacial troughs, *Oceanologia*, **51**, 321–340.

Mauritzen, C., S. S. Hjøllo, and A. B. Sandø, 2006: Passive tracers and active dynamics: A model study of hydrography and circulation in the northern North Atlantic, *J. Geophys. Res.*, **111**, C08014, doi:10.1029/2005JC003252.

Mork, K.A., and J. Blindheim, 2000: Variations in the Atlantic infow to the Nordic Seas, 1955-1996, *Deep-Sea Res. I*, **47**, 1035-1057.

Overland, J.E., M. Wang, and S. Salo, 2008: The recent Arctic warm period, *Tellus,* **60A**, 589–597.

Orvik, K.A., and P. Niiler 2002: Major pathways of Atlantic water in the northern North Atlantic and Nordic Seas toward Arctic, *Geophys. Res. Letts.*, **29**, 1896, doi:10.1029/2002GL015002.

Piechura, J., and W. Walczowski, 2009: Warming of the West Spitsbergen Current and sea ice north of Svalbard, *Oceanologia*, **51**, 147–164.

Podesta, G.P., M. Arbelo, R. Evans, K. Kilpatrick, V. Halliwell, and J. Brown, 2003: Errors in high-latitude SSTs and other geophysical products linked to NOAA-14 AVHRR channel 4 problems, *Geophys. Res. Letts*.,**30**, 1548, doi:10.1029/2003GL017178.

Polyakov, I.V., G.V. Alekseev, L.A. Timokhov, U. S. Bhatt, R.L. Colony, H.L. Simmons, D. Walsh, J. E. Walsh, and V. F. Zakharov, 2004: Variability of the intermediate Atlantic water of the Arctic Ocean over the last 100 years, *J. Clim.*, **17**, 4485– 4497.

Reynolds, R.W., T.M. Smith, C. Liu, D.B. Chelton, K.S. Casey, and M.G. Schlax, 2007: Daily High-Resolution-Blended Analyses for Sea Surface Temperature, *J. Clim.*, **20**, 5473-5496.

Saloranta T.M., and P.M. Haugan, 2001: Interannual variability in the hydrography of Atlantic water northwest of Svalbard, *J. Geophys. Res.*, **106**, 13,931-13,943.

A. B. Sandø, A.B., and T. Furevik, 2008: Relation between the wind stress curl in the North Atlantic and the Atlantic inflow to the Nordic Seas, *J. Geophys. Res.*, **113**, C06028, doi:10.1029/2007JC004236.

Schauer, U., Loeng H., Rudels B., Ozhigin V. K., Dieck W., 2002: Atlantic water flow through the Barents and Kara Seas, *Deep-Sea Res. I*, **49**, 2281–2298.

Schauer, U., E. Fahrbach, S. Osterhus, and G. Rohardt, 2004: Arctic warming through the Fram Strait: Oceanic heat transport from 3 years of measurements, *J. Geophys. Res.*, **109**, C06026, doi:10.1029/ 2003JC001823.

Schlichtholz, P., and I. Goszczko, 2006: Interannual variability of the Atlantic water layer in the West Spitsbergen Current at 76.5^{o}N in summer 1991–2003, *Deep-Sea Res. I*, **53**, 608–626.

Semenov, V.A., W. Park, and M. Latif, 2009: Barents Sea inflow shutdown: A new mechanism for rapid climate changes, *Geophys. Res. Letts.*, **36**, L14709, doi:10.1029/2009GL038911.

Skagseth Ø., T. Furevik, R. Ingvaldsen, H. Loeng, K.A. Mork, K.A. Orvik, V. Ozhigin, 2008, Volume and heat transports to the Arctic Ocean via the Norwegian and Barents Seas, in: Arctic–subarctic ocean fluxes defining the role of the Northern Seas in climate, R.R. Dickson, J. Meincke & P. Rhines (eds.), Springer, Dordrecht, 45–62.

Smolyar I., and N. Adrov, 2003: The quantitative definition of the Barents Sea Atlantic water: mapping of the annual climatic cycle and interannual variability, *ICES J. Marine Sci.*, **60**, 836–845.

Steele, M., R. Morley, and W. Ermold, 2001: PHC: A global ocean hydrography with a high quality Arctic Ocean, *J. Clim.*, **14**, 2079– 2087.

Swift, J.H., E.P. Jones, K. Aagaard, E.C. Carmack, M. Hingston, R.W. MacDonald, F.A. McLaughlin, and R.G. Perkin, 1998: Waters of the Makarov and Canada basins, *Deep Sea Res. I*, **44**, 1503-1529.

Swift, J.H., K. Aagaard, L. Timokhov, and E. G. Nikiforov, 2005: Long-term variability of Arctic Ocean waters: Evidence from a reanalysis of the EWG data set, *J. Geophys. Res.*, **110**, C03012, doi:10.1029/2004JC002312.

Uppala, S.M., et al, 2005: the ERA-40 reanalysis, *Q.J.R. Meteorol. Soc.*, **131**, 2961-3012.

Walczowski, W. and J. Piechura, 2006: New evidence of warming propagating toward the Arctic Ocean, *Geophys. Res. Letts*., **33**, L12601, doi:10.1029/2006GL025872.

Yu, L., X. Jin, and R. A. Weller, 2008: Multidecade Global Flux Datasets from the Objectively Analyzed Air-sea Fluxes (OAFlux) Project: Latent and sensible heat fluxes, ocean evaporation, and related surface meteorological variables. Woods Hole Oceanographic Institution, OAFlux Project Technical Report. OA-2008-01, 64pp. Woods Hole, Massachusetts.

Zhang, J., D.A. Rothrock, and M. Steele, 1998: Warming of the Arctic Ocean by a strengthened Atlantic inflow: model results, *Geophys. Res. Letts.,* **25**, 1745–1748.

Figure Legends

Figure 1 Time mean temperature (contours) and salinity (colors) for the 60-year period 1950-2009 at 100m depth. The Nordic Seas Atlantic Water Zone (AWZ) used in subsequent calculations is defined as the area circumscribed by the 35psu contour north of 63^{o}N. The Fram Strait (ABC) and Barents Sea (ABD) transects are indicated as well. Upper left and lower right insets shows salinity (psu) and temperature (^{o}C) as a function of depth (m) averaged over the AWZ. Summer (July-October) in red and winter (January-May) in blue.

Figure 2. (a) Number of temperature (black) and salinity (green) observations in the sector 50^{o}W-80^{o}E, 60^{o}N-90^{o}N with time at 100m 1950-2009. Insets show monthly average and vertical distribution of temperature and salinity observations. (b) Spatial distribution of temperature (left) and salinity (right) observations per 100km^2 square 1950-2009. Insets show monthly average and vertical distribution of temperature and salinity observations.

Figure 3. Time mean temperature (solid contours), potential density (dashed contours), and salinity (colors) for the 60-year period 1950-2009 computed in a 2^{o} wide band perpendicular to the track along the Fram Strait (ABC, upper panel) and Barents Sea (ABD, lower panel) transects and plotted as a function of depth and distance along transect in kilometers.

Figure 4 Annual temperature, salinity, and potential density anomalies from their 60-year mean in the AWZ as a function of depth and time. Four warm periods and three cold periods are indicated. Seasonal profiles of temperature and salinity are provided in **Fig. 1**.

Figure 5 Geographic structures of temperature and salinity anomalies relative to the climatological monthly cycle at 100m depth for the four warm events (shading). Contours show the AWZ for the individual events (bold) and the mean position of the AWZ (thin). Regions with insufficient data sampling are shaded light grey.

Figure 6 Geographic structures of temperature and salinity anomalies relative to the climatological monthly cycle at 100m depth for the three cold events (shading). Contours show the AWZ for the individual events (bold) and the mean position of the AWZ (thin). Regions with insufficient data sampling are shaded light grey.

Figure 7. Upper and middle panels show SST anomaly for summer (May-Oct) and winter (Nov-Apr) during W4 (March 1999 - December 2009) relative to the climatological monthly cycle 1982-2009. Lowest panel shows time series of monthly anomalies averaged over the extended domain 60^{o}W-80^{o}E, 40^{o}N-90^{o}N (excluding marginal seas). Colors highlight (red) summer and (blue) winter seasons.

Figure 8 (upper panel) Annual heat content anomalies ($HC = \rho C_p \int_{600}^{0} T' dz$) integrated throughout the AWZ (where T' is anomalous temperature). Grey line shows the two-year smoothed monthly NAO Index time series obtained from the National Centers for Environmental Prediction (vertical range: ±0.8). (middle panel) Biannually smoothed rate of heat storage anomalies ($\partial HC / \partial t$, black) and four estimates of net surface heat flux averaged over the AWZ: NCAR/NCEP reanalysis (blue), ERA-40 (red), ERA-Interim (yellow), and WHOI (green). Downward heat flux into the ocean is positive. (Lower panel) Convergence of horizontal heat transport, estimated as the difference between net surface heat flux and rate of heat storage, for each surface heat flux estimate.

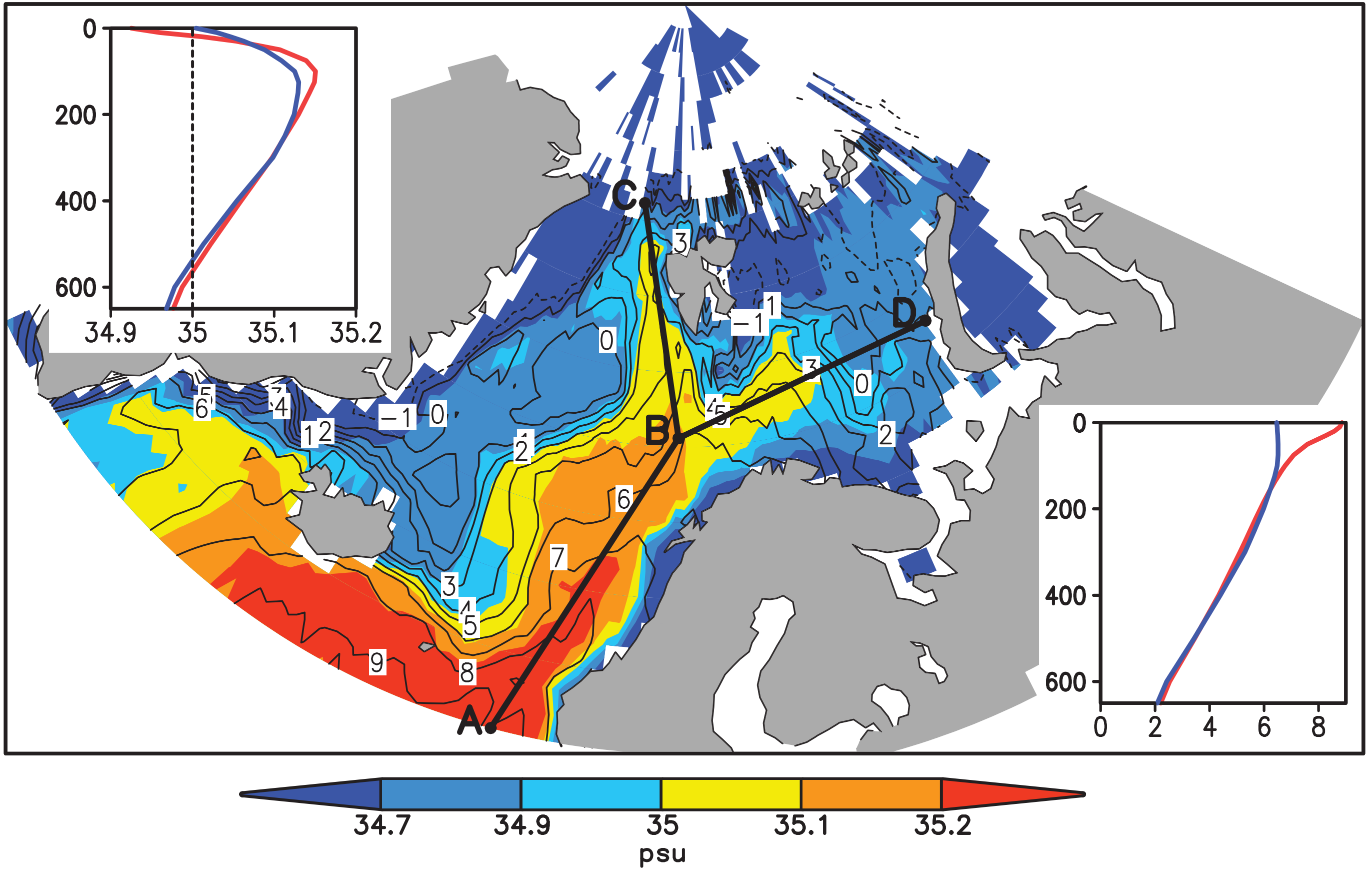

0
200
400
600
34.9
35
35.1
35.2
C
B
A
D
0
200
400
600
0
2
4
6
8
34.7
34.9
35
35.1
35.2
psu

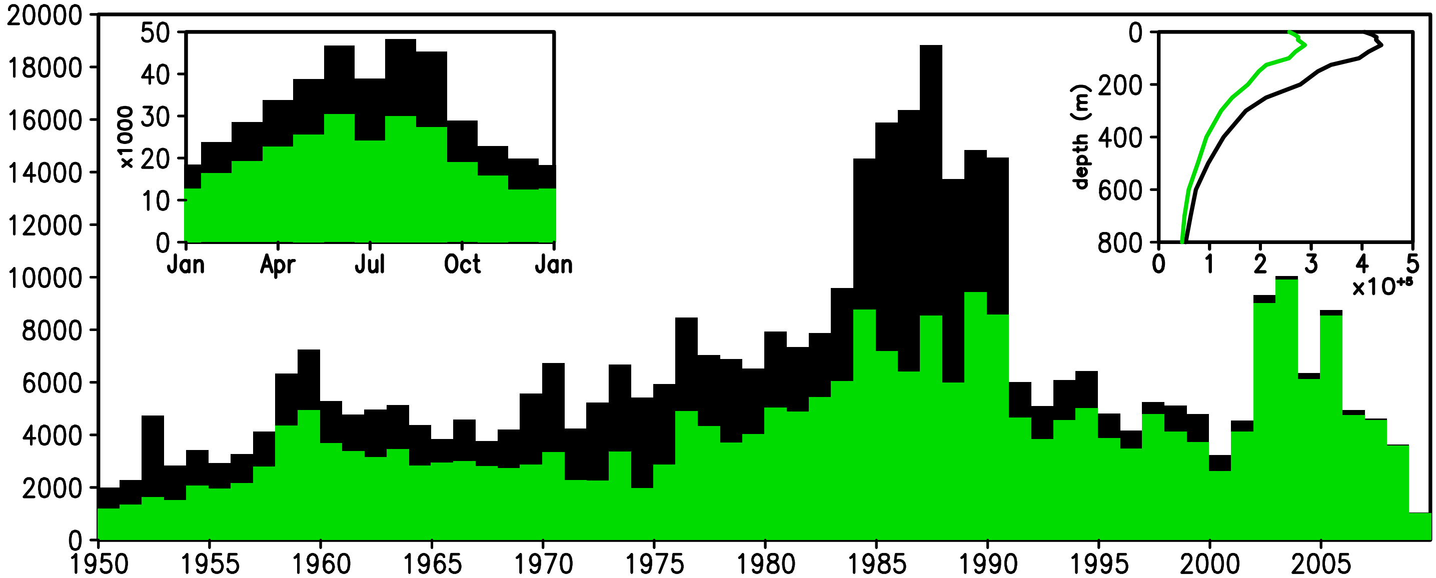

1950–2009, 100m

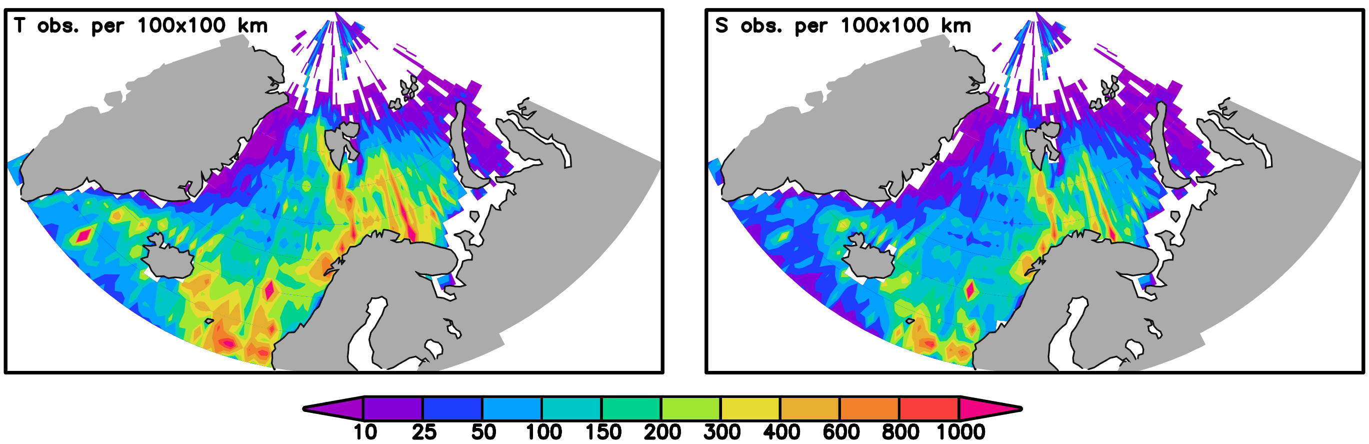

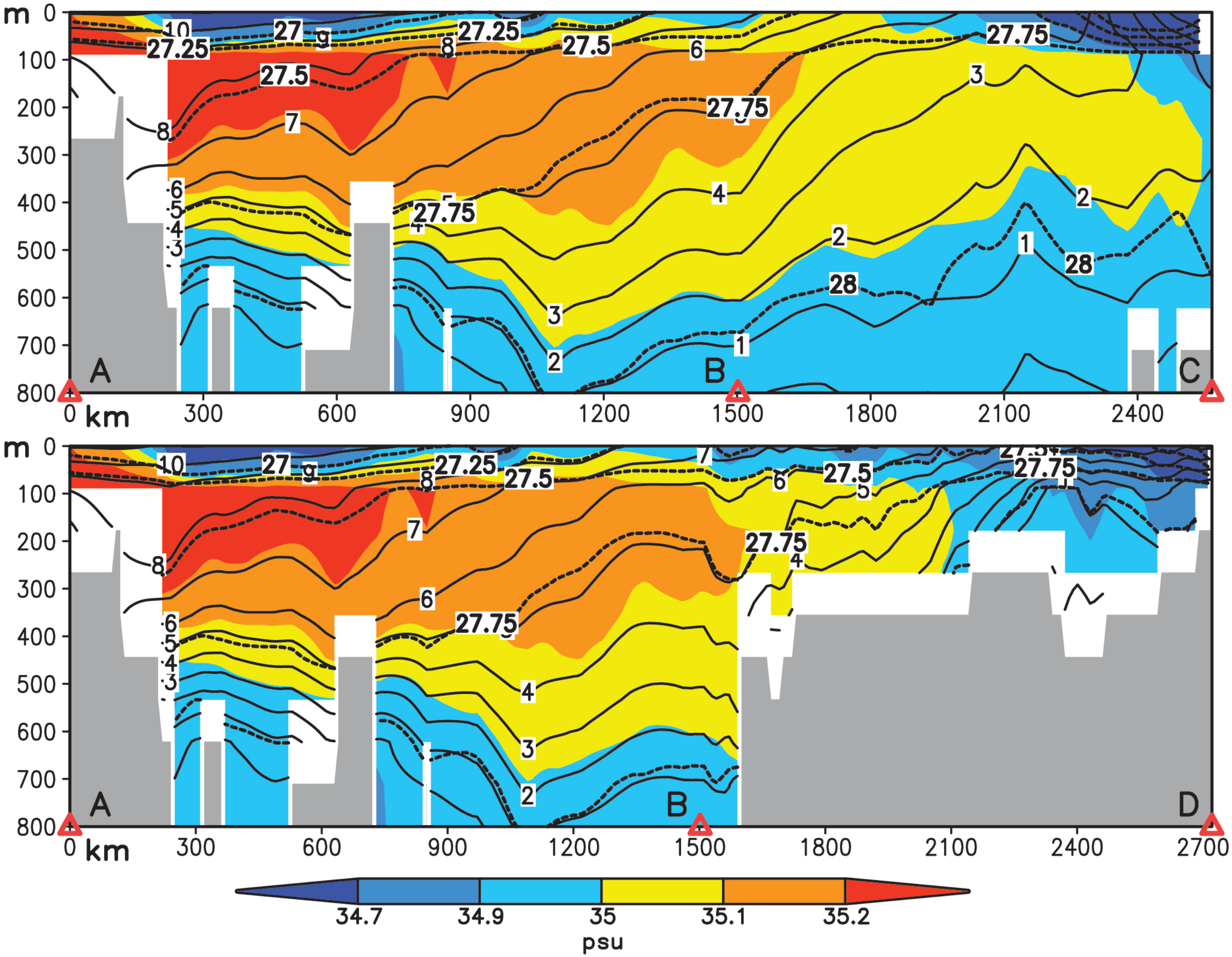

m
0
100
200
300
400
500
600
700
800
0 km
300
600
900
1200
1500
1800
2100
2400
2700
A
B
C
D
27
27.25
27.5
27.75
28
10
8
7
6
5
4
3
2
1
34.7
34.9
35
35.1
35.2
psu

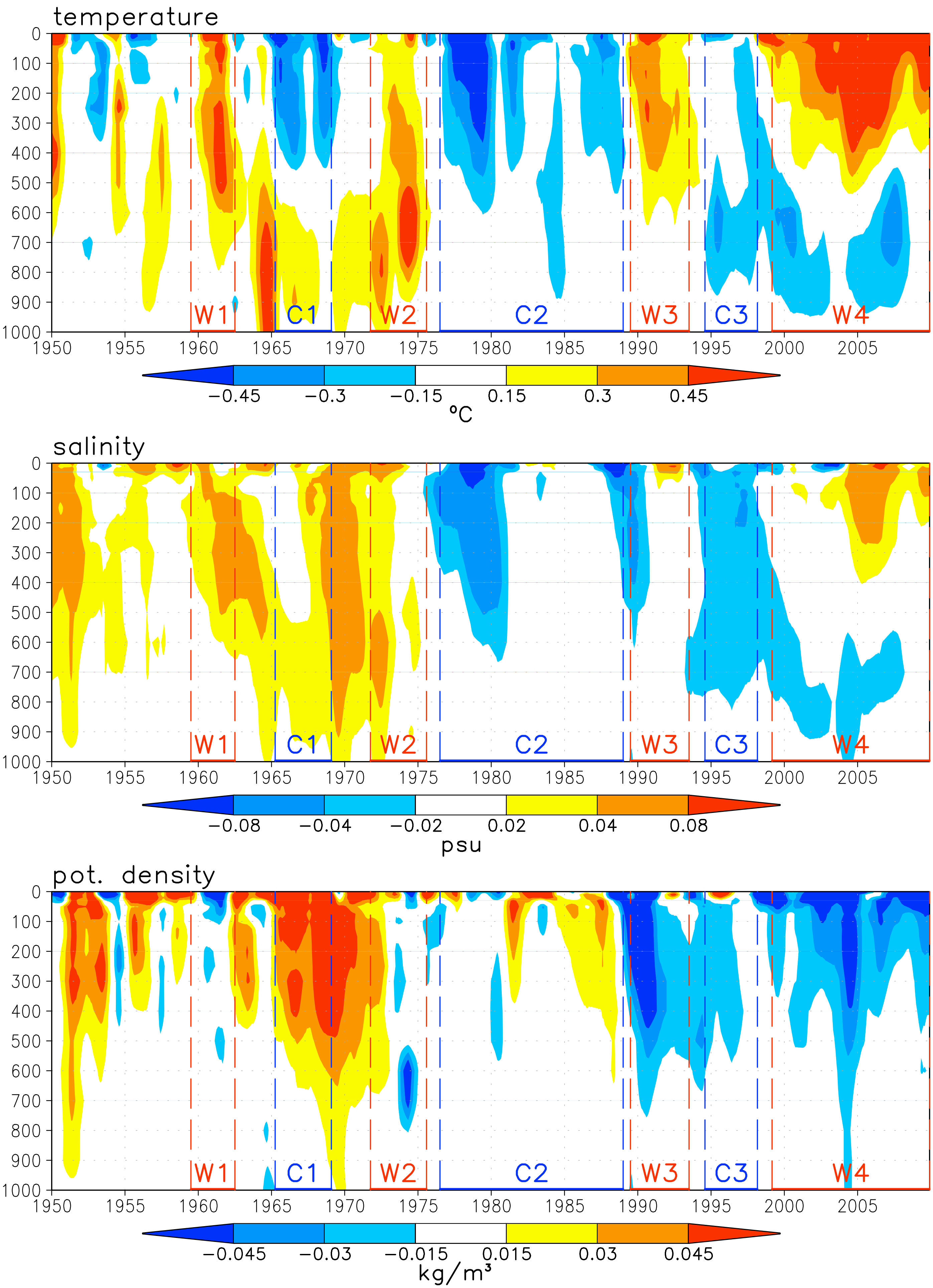
temperature
0
100
200
300
400
500
600
700
800
900
1000
1950
1955
1960
1965
1970
1975
1980
1985
1990
1995
2000
2005
W1
C1
W2
C2
W3
C3
W4
−0.45
−0.3
−0.15
0.15
0.3
0.45
°C
salinity
−0.08
−0.04
−0.02
0.02
0.04
0.08
psu
pot. density
−0.045
−0.03
−0.015
0.015
0.03
0.045
kg/m³

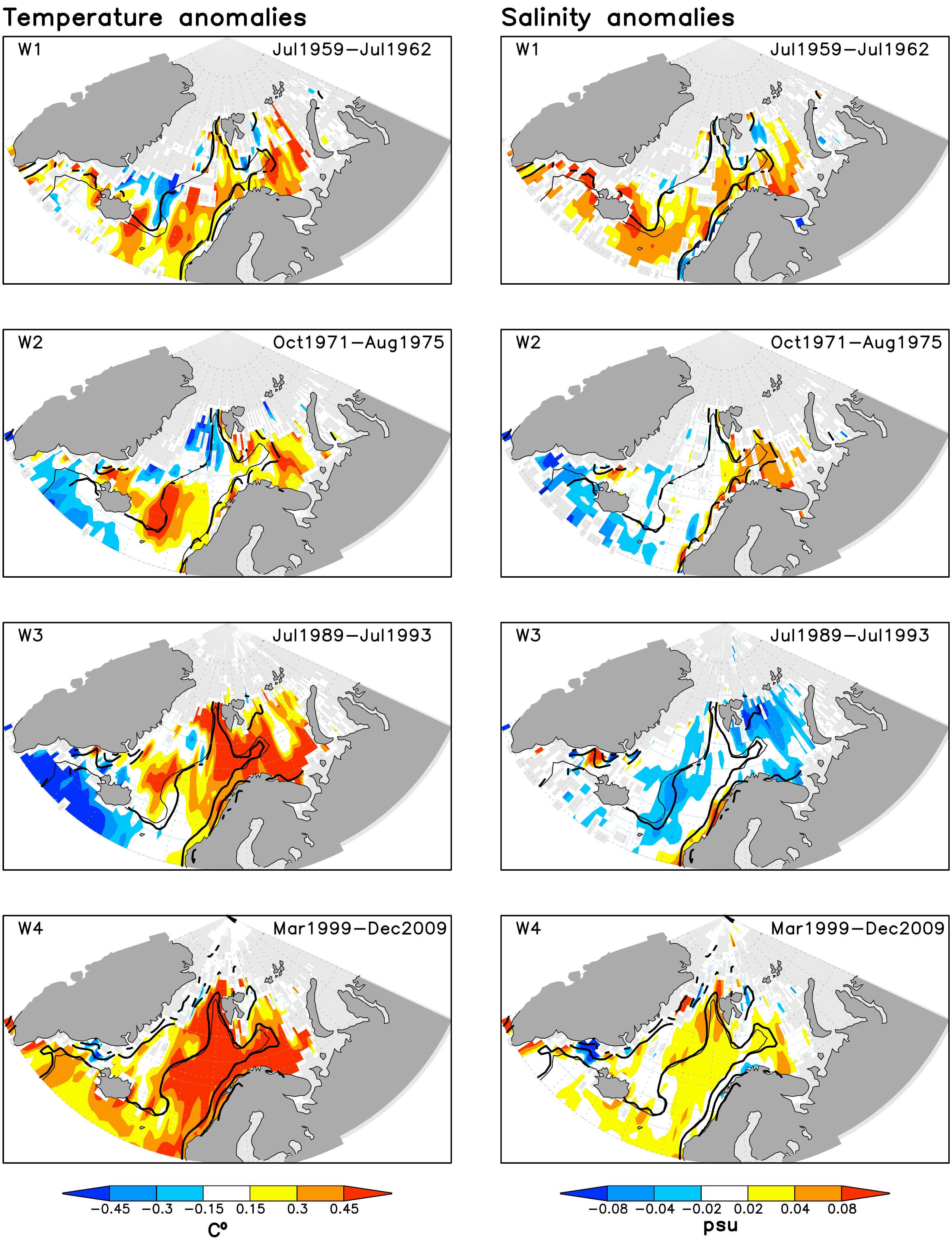
Temperature anomalies
Salinity anomalies
W1
Jul1959–Jul1962
W2
Oct1971–Aug1975
W3
Jul1989–Jul1993
W4
Mar1999–Dec2009
−0.45 −0.3 −0.15 0.15 0.3 0.45
C°
−0.08 −0.04 −0.02 0.02 0.04 0.08
psu

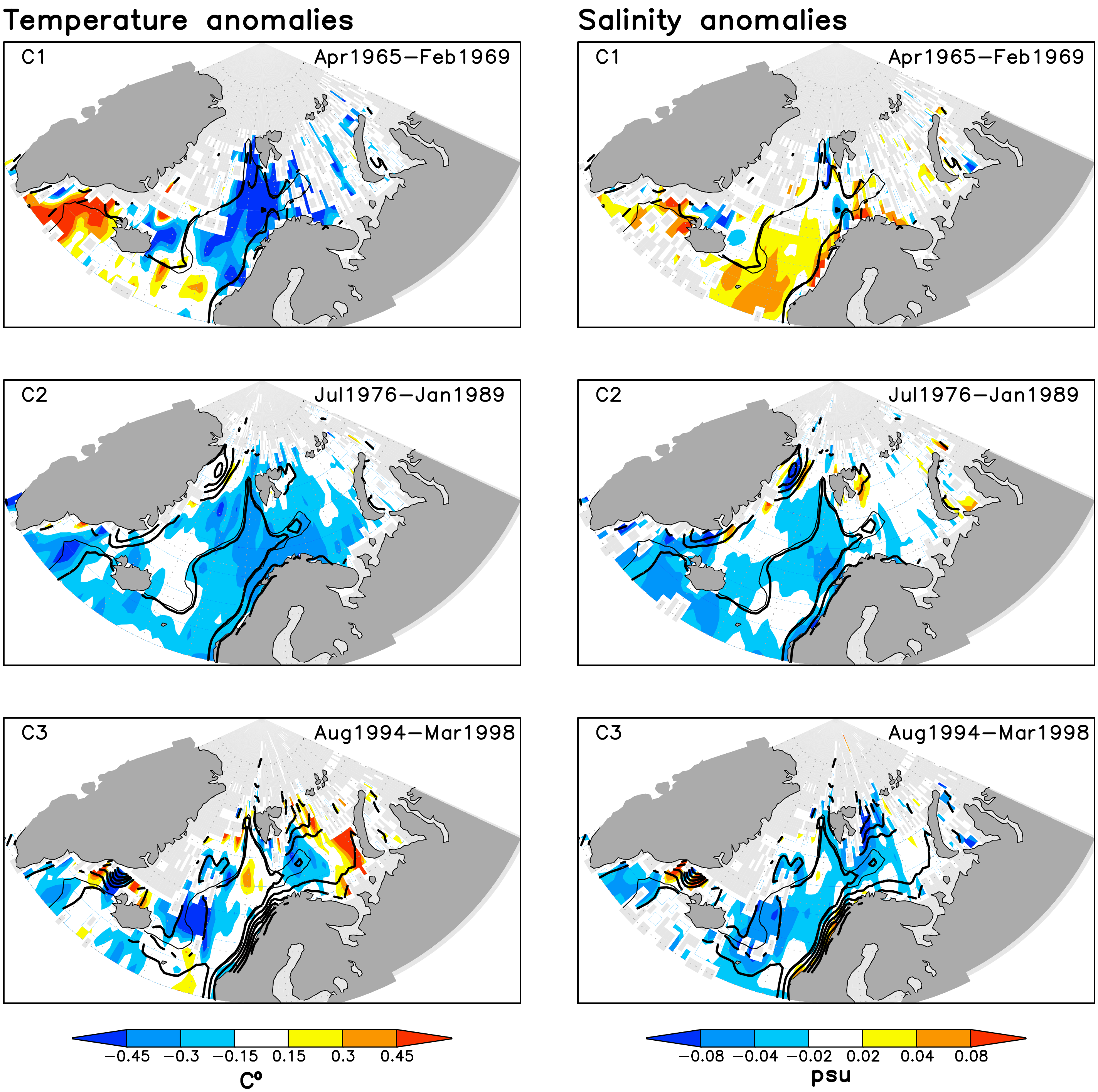
Temperature anomalies
Salinity anomalies
C1
Apr1965–Feb1969
C2
Jul1976–Jan1989
C3
Aug1994–Mar1998
−0.45 −0.3 −0.15 0.15 0.3 0.45
C°
−0.08 −0.04 −0.02 0.02 0.04 0.08
psu

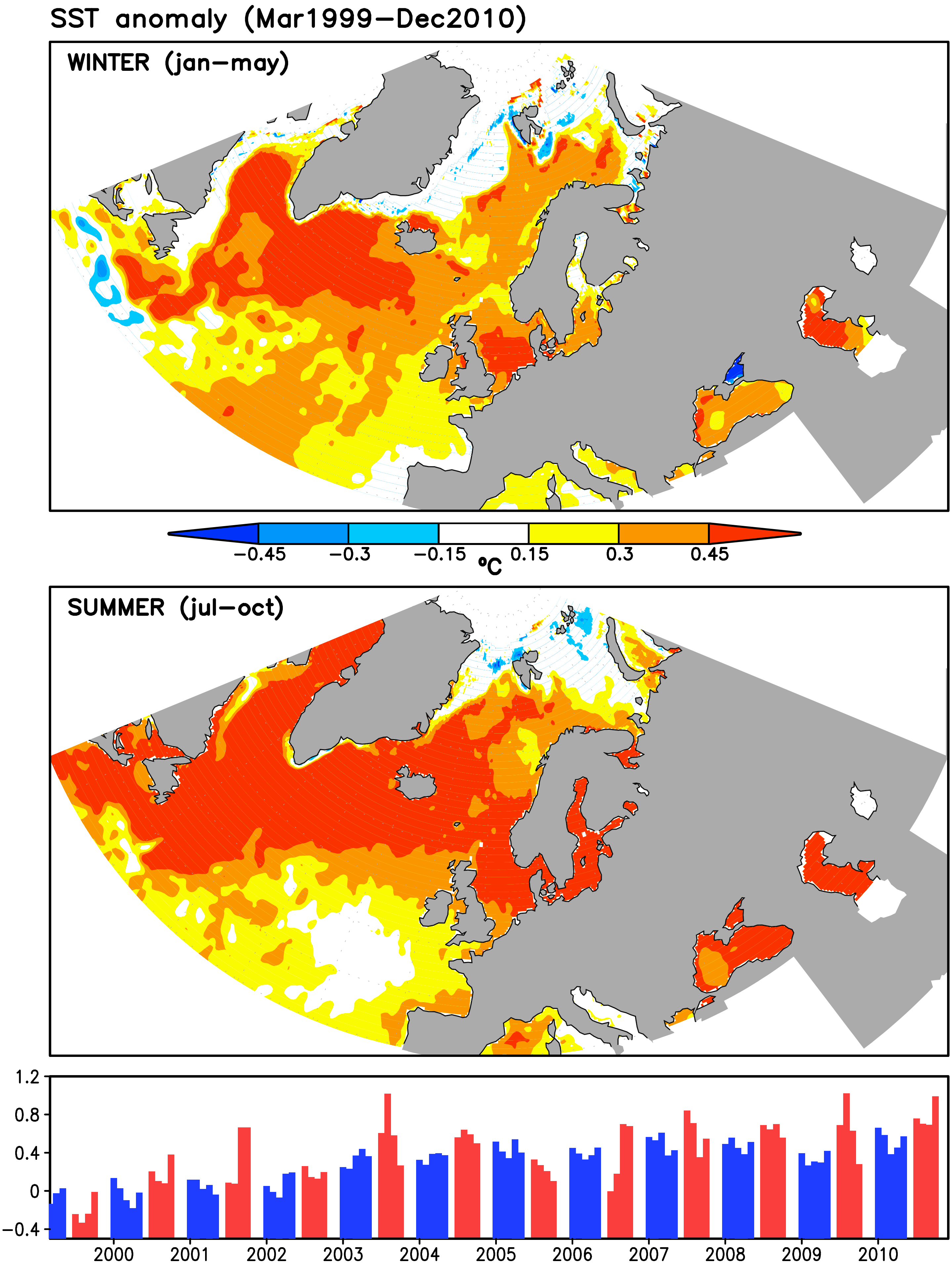

SST anomaly (Mar1999–Dec2010)
WINTER (jan–may)
−0.45
−0.3
−0.15
0.15
0.3
0.45
°C
SUMMER (jul–oct)
1.2
0.8
0.4
0
−0.4
2000
2001
2002
2003
2004
2005
2006
2007
2008
2009
2010

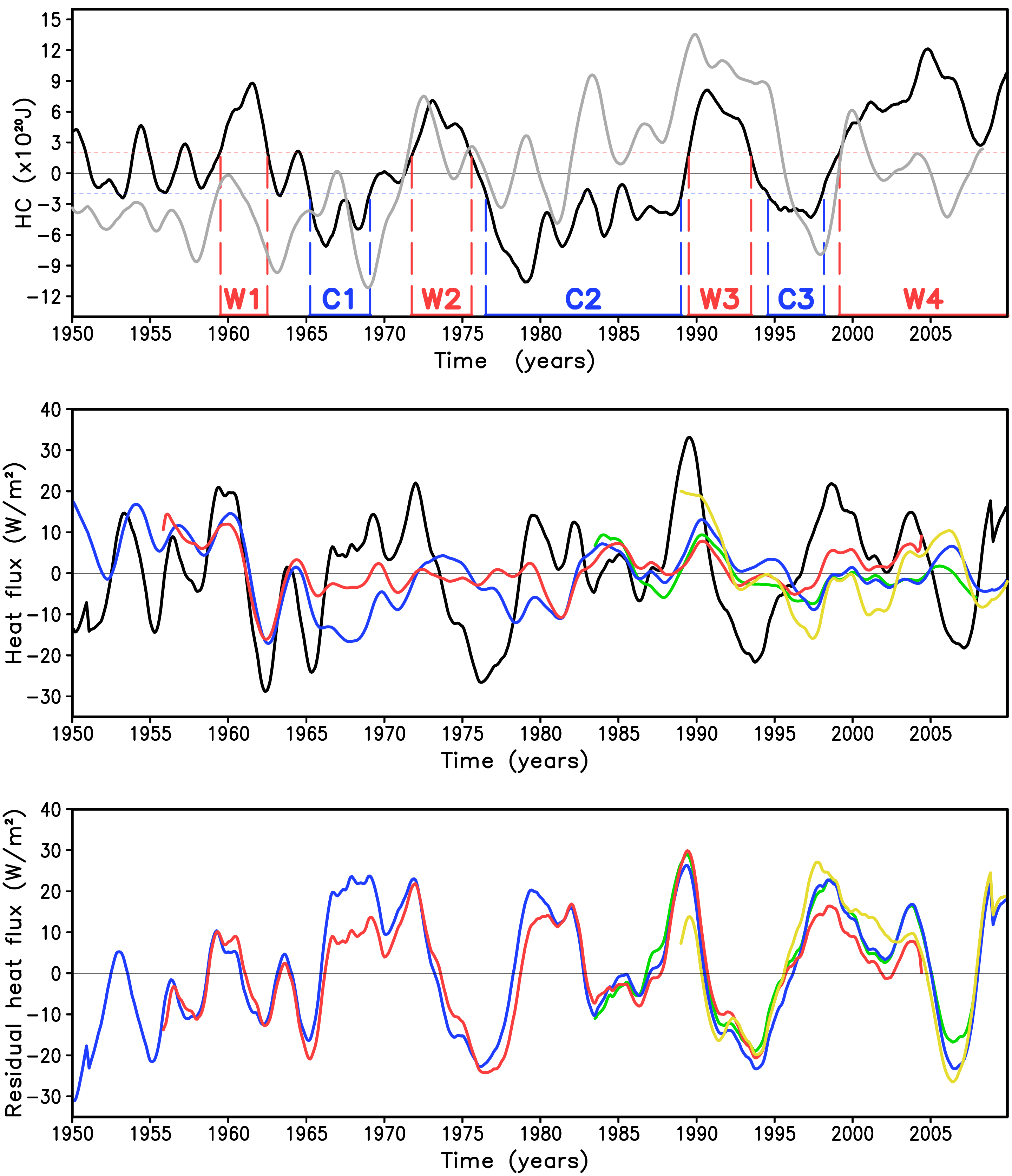

HC (x10^{20}J)
15
12
9
6
3
0
−3
−6
−9
−12
W1
C1
W2
C2
W3
C3
W4
1950
1955
1960
1965
1970
1975
1980
1985
1990
1995
2000
2005
Time (years)
Heat flux (W/m^2)
40
30
20
10
0
−10
−20
−30
Time (years)
Residual heat flux (W/m^2)
Time (years)